

## High-Power Microwaves from a Nonisochronic Reflecting Electron System

R. A. Mahaffey, P. Sprangle, J. Golden, and C. A. Kapetanakos

Naval Research Laboratory, Washington, D. C. 20375

(Received 7 April 1977)

High-power microwave radiation is observed when a positive pulse is applied to an anode of a reflex triode. The frequency of radiation varies as  $f \sim V^{1/2}/D^n$ , where  $V$  is the anode voltage,  $D$  is the cathode-virtual-cathode spacing, and  $0 < n \leq 1$ . The basic features of the radiation are explained by a theoretical model which predicts particle bunching as a result of the energy dependence of the electron oscillation frequency.

Reflecting electron systems in the form of a low-inductance, coaxial reflex triode have been recently used to produce MeV proton pulses<sup>1</sup> of peak current in excess of 200 kA. In the Letter, we report results which demonstrate that reflecting electron systems can generate high-power microwaves with or without an applied axial magnetic field ( $B_0$ ). The microwave emission is attributed to the phase bunching of the oscillating electrons inside the potential well of the system. This bunching is due to the energy ( $\epsilon$ ) dependence of the electron oscillation frequency  $\omega_0$ . For the idealized parabolic potential well of Fig. 1(a),  $\omega_0$  is a function of  $\epsilon$  only for relativistic electrons. In the presence of an oscillatory electric field  $E = E_0 \cos(\omega t)$  of frequency  $\omega \gtrsim \omega_0$ , a sample of initially uniformly distributed electrons will be bunched as shown in Fig. 1(b). The reason for this bunching is that  $\partial\omega_0/\partial\epsilon < 0$  and thus those electrons located in the upper half-plane at  $t = 0$  gain energy ( $\omega_0$  increases) and their phase advances ahead of the wave. This nonisochronic mechanism is similar to that of the electron cyclotron maser.<sup>2,3</sup> As will become apparent later on, reflecting electron systems have some distinct advantages over several of the previously reported devices that also use relativistic electron beams<sup>4-9</sup> for the generation of microwaves.

In its simplest form, a reflecting electron system (see Fig. 1) consists of a positively biased, semitransparent anode and a grounded cathode.<sup>10</sup> Electrons emitted from the cathode are accelerated by the positive pulse that is applied to the anode, pass through it, and form a virtual cathode. In general, the virtual cathode is formed at a distance from the anode that is different from the anode-cathode opening ( $d$ ). As a result of the positive potential on the anode, the electrons do not leave the system but rather oscillate between the real and virtual cathodes.

The experimental setup has been described previously in connection with the generation of intense, pulsed ion beams.<sup>11,12</sup> Briefly, the 50-

nsec duration, 250–350-kV positive pulse from a 7- $\Omega$  generator is applied to the anode of a reflex triode. The anode is made either from 6- $\mu$ m-thick aluminized Mylar or bare, parallel copper wires spaced 2 cm apart. It has been determined in previous experiments that with these sorts of anodes the ion flux generated by the device is very small. Both the power and the frequency of the emitted microwaves appear to be sensitive to the shape of the cathode. The maximum power was obtained at  $B_0 = 0$  with an 8.4-cm o.d. solid cathode facing an aluminized Mylar anode for  $d = 1.2$  cm.

The emitted microwave radiation is monitored in both the X band ( $f = 8.2$ – $12.4$  GHz) and the Ka band ( $f = 26.5$ – $40$  GHz). The horn antennas are situated about 26 cm from the anode with their axes either parallel to the direction of the accelerating electric field (end-on) or with their axes perpendicular to it (side-on). A very small portion of the microwave signal taken from the output of a directional coupler which is located immediately after the horn is fed almost undis-

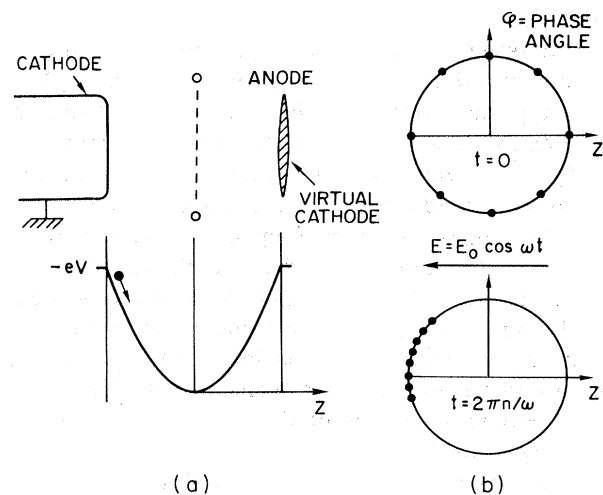


FIG. 1. (a) Reflex triode and idealized potential well; (b) phase bunching of electrons after several periods when  $\omega \gtrsim \omega_0$ .

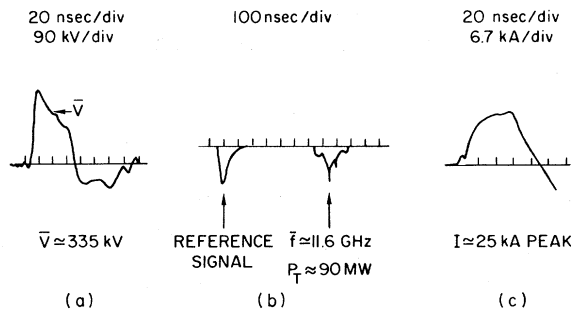


FIG. 2. Typical wave forms: (a) Voltage at 90 kV/div; (b) X-band microwaves. The reference signal has been delayed by 554 nsec; and (c) electron current at 7 kA/div. The origin of sharp spikes in (b) is not presently well understood.

persed to an oscilloscope and is used as a time marker. The rest of the microwave signal is transmitted through a long (323 m in the X band, 60 m in the Ka band) dispersive line and is also fed to the same oscilloscope. The time delay between the two signals gives information about the frequency spectrum of the radiation.<sup>13</sup> Typical dispersed signals are shown in Fig. 2 together with the voltage pulse applied to the anode and the current flowing in the device. Since the power of the X-band radiation is about equal at the only two accessible positions of the system that are located about 90° apart, it is reasonable to assume that the emitted radiation is isotropic. Extrapolating the power measured at the horn under the above assumption, the power emitted by the device at a single frequency over a 4π solid angle is between 90 and 100 MW, corresponding to an efficiency of about 1.5%.

A striking feature of the experimental results is the variation of the microwave frequency ( $f$ ) with applied voltage ( $V$ ) shown in Fig. 3. Clearly, the central frequency  $f_c$  of the spectrum varies as  $f_c \sim \bar{V}^{1/2}$ , where  $\bar{V}$  is the time-averaged anode potential. In addition, the results of Fig. 3 show that the frequency depends upon the shape of the cathode. It can be shown that the distance between the virtual cathode and anode decreases as the thickness of an annular cathode increases. Since the frequency of radiation  $f \sim h\tau_t^{-1}$ , where  $h$  is an integer and  $\tau_t$  is the transit time of a typical electron in the potential well, higher frequencies are expected with higher voltages and shorter openings between the real and virtual cathodes. As the anode is moved closer to the real cathode, the spacing between the anode and the virtual cathode is also reduced and, thus, higher fre-

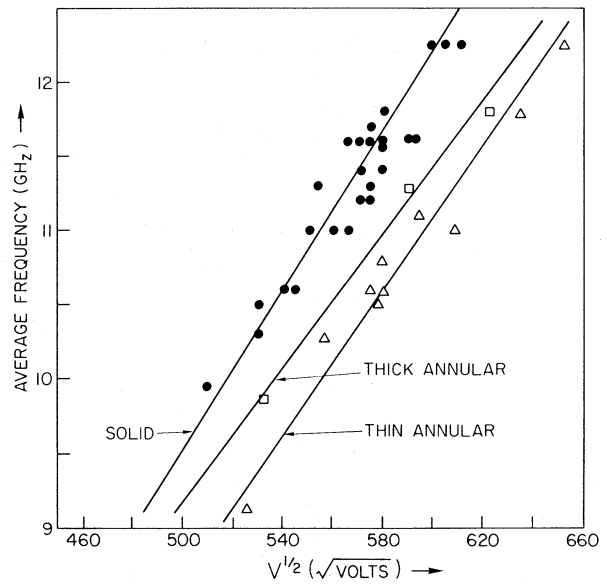


FIG. 3. Average frequency vs the square root of the averaged applied voltage for three different cathodes of areas 55 cm<sup>2</sup> (solid), 89 cm<sup>2</sup> (thick annular), and 51 cm<sup>2</sup> (thin annular).

quencies are expected. This is shown in Fig. 4.

The voltage dependence of the microwave frequency can also explain the frequency spread of the signal shown in Fig. 2. For this particular shot the voltage pulse drops by 150 kV during its duration, corresponding to a  $\Delta V/V \approx 0.4$  or to  $\Delta\sqrt{V}/\sqrt{V} \approx 0.2$ , which is about equal to the ob-

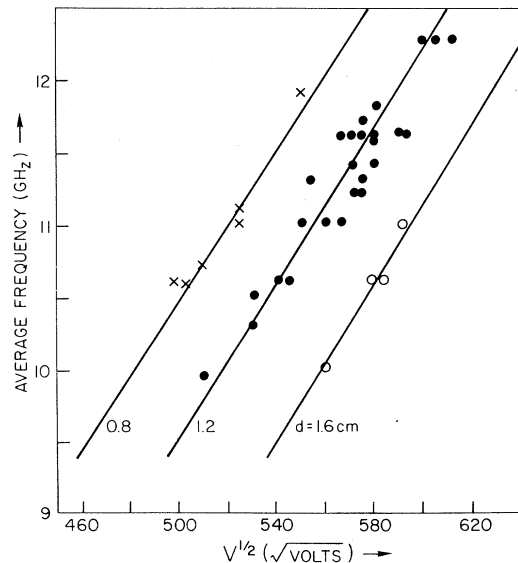


FIG. 4. Average frequency vs the square root of the averaged applied voltage for three anode-cathode spacings.

served  $\Delta f/f$ .

At  $B_0 = 0$ , with an aluminized Mylar anode located 1.2 cm away from a solid carbon cathode, the  $Ka$ -band power of the microwave radiation at the horn located about 26 cm from the anode with its axis parallel to the accelerating field is about 5 KW. This corresponds to a total power emitted over the  $4\pi$  solid angle of more than 10 MW. Prior to detection, the signal is passed through a 60-m-long dispersive line and the observed time delay of 230 nsec corresponds to a central frequency of 36.6 GHz.

A drastic reduction in the X-band microwave power is observed when the reflex triode is immersed in an external axial magnetic field. The emitted power shows a resonancelike behavior with the applied field. The power at the peak of the resonance is about two orders of magnitude lower than the corresponding power at  $B_0 = 0$ . In addition, the frequency of the emitted radiation increases approximately linearly with the value

$$\Delta W_{KE} = W_{KE}(t) - W_{KE}(t_0) \\ = \frac{|e|2n_0\hat{E}^2\omega_0}{2(\Delta\omega_1)^2} \left\{ \omega_0 \frac{\partial |\hat{z}_1|^2}{\partial \epsilon} (1 - \cos\Delta\omega_1\tau) + |\hat{z}_1|^2 \frac{\partial \omega_0}{\partial \epsilon} \left[ \left(1 + \frac{2\omega_0}{\Delta\omega_1}\right) (1 - \cos\Delta\omega_1\tau) - \omega_0\tau \sin\Delta\omega_1\tau \right] \right\}, \quad (1)$$

where  $n_0$  is the average electron density,  $\Delta\omega_1 = \omega - l\omega_0$ , and  $\tau = t - t_0$ .

If  $\Delta W_{KE} > 0$  the perturbing wave is absorbed by the oscillating particles, while if  $\Delta W_{KE} < 0$  the particles lose kinetic energy to the wave resulting in wave growth. The term on the right-hand side of Eq. (1) which contains the quantity  $\partial |\hat{z}_1|^2 / \partial \epsilon$  is always positive and hence is a stabilizing term.

The remaining term which is proportional to  $\partial \omega_0 / \partial \epsilon$ , however, can be negative depending on the sign of  $\partial \omega_0 / \partial \epsilon$  and  $\Delta\omega_1$ . It is this term which gives rise to the growth of the wave. It can be shown from Eq. (1) that the condition for the initial growth of the wave is that

$$(\Delta\omega_1)^{-1} \partial \omega_0 / \partial \epsilon < 0, \quad (2a)$$

together with

$$\frac{\partial |\hat{z}_1|^2}{\partial \epsilon} < - \frac{|\hat{z}_1|^2}{\Delta\omega_1} \frac{\partial \omega_0}{\partial \epsilon}. \quad (2b)$$

The particle oscillations are nonisochronous,  $\partial \omega_0 / \partial \epsilon \neq 0$ , if the potential well is nonparabolic and/or the particles are relativistic. In the present experiment both of these situations are satisfied. Using the wave equation for  $E^{(1)}$  an approxi-

mate dispersion relation has been derived, which in the neighborhood of the unstable frequency takes the form

$$(\Delta\omega_1)^3 - \omega_b^2 \omega_0 m_0 (\partial / \partial \epsilon) (\omega_0 |\hat{z}_1|^2) \Delta\omega_1 / 2 \\ = (\omega_b^2 \omega_0^2 m_0 |\hat{z}_1|^2 / 2) \partial \omega_0 / \partial \epsilon, \quad (3)$$

where  $\omega_b^2 = 4\pi |e|^2 n_0 / m_0$ .

As an illustration we consider the simplified situation where the particles are mildly relativistic and the potential is parabolic given by  $E^{(0)}(z^{(0)}) = \xi_0 z^{(0)}$  where  $\xi_0$  is a constant. To lowest order in the small parameter  $\epsilon / m_0 c^2$  we find that

$$\omega_0 = \alpha_0 \left(1 - \frac{3}{8} \epsilon / m_0 c^2\right),$$

and

$$|\hat{z}_1|^2 = (c^2 / 2\alpha_0^2) \epsilon / m_0 c^2, \quad (4)$$

where  $\alpha_0 = |e| \xi_0 / m_0$  is the nonrelativistic particle oscillation frequency in a parabolic potential. Using Eq. (4) in the expression for the dispersion relation we find that a threshold condition for instability exists and is

$$\epsilon / m_0 c^2 > (8/9\sqrt{3}) \omega_b / \alpha_0. \quad (5)$$

If the inequality in (5) is satisfied, Eq. (3) can be solved for the linear growth rate  $\Gamma = -\text{Im}(\Delta\omega_1)$  and frequency shift  $\delta\omega = \text{Re}(\Delta\omega_1)$ , which are

$$\Gamma = \frac{\sqrt{3}}{4} \left(\frac{3}{4}\right)^{1/3} (\omega_b^2 \alpha_0)^{1/3} (\epsilon/m_0 c^2)^{2/3} = \sqrt{3} \delta\omega. \quad (6)$$

This idealized theoretical model predicts that bunching occurs and gives the qualitative dependence of the emitted frequency on the transit time, which is consistent with the observation that  $f \sim V^{1/2}/D^n$ .

It is apparent from the previous discussion that nonisochronic reflecting electron systems have five interesting features: (i) that the emitted power is maximum when  $B_0 = 0$ ; (ii) compactness; (iii) tunability; (iv) monochromaticity; and (v) long pulse time. It is possible that the emitted radiation could be used to furnish information about the properties of the device. For instance, the electron density may be determined from the threshold condition given in Eq. (5). However, this equation has been derived under idealized conditions and thus its application to obtain plasma properties is not presently warranted. Therefore, the emitted radiation will be used as a diagnostic tool after the development of more complete, self-consistent models that are based on arbitrary potential-well shapes. Presently, an experiment is under way to measure the anode-virtual cathode opening from the frequency of the emitted radiation. Preliminary results are very encouraging and will be reported in the near future.

It is very likely the mechanism responsible for the generation of microwave radiation in our sys-

tem is also responsible for the high-power (more than 1 GW) X-band radiation observed by Doucet and Buzzi,<sup>14</sup> when a 400-kV, 100-kA relativistic electron beam is injected into a vacuum through a foil anode.

One of us (R.A.M.) is a National Research Council Research Associate at the Naval Research Laboratory.

<sup>1</sup>J. Golden, C. A. Kapetanakis, S. J. Marsh, and S. J. Stephanakis, *Phys. Rev. Lett.* **38**, 130 (1977).

<sup>2</sup>A. V. Gapanov, M. I. Petelin, and V. K. Yulpatov, *Izv. Vyssh. Uchebn. Zaved. Radiofiz.* **10**, 1414 (1967).

<sup>3</sup>P. Sprangle and A. T. Drobot, *Proc. IEEE Special Issue on Sub-Millimeter Radiation* (IEEE, New York, 1977), p. 65, and references therein.

<sup>4</sup>M. Friedman and M. Herndon, *Phys. Rev. Lett.* **28**, 210 (1972).

<sup>5</sup>M. Friedman, D. A. Hammer, W. M. Manheimer, and P. Sprangle, *Phys. Rev. Lett.* **31**, 752 (1973).

<sup>6</sup>G. Bekefi and T. J. Orzekowski, *Phys. Rev. Lett.* **37**, 379 (1976).

<sup>7</sup>J. A. Nation, *Appl. Phys. Lett.* **17**, 491 (1970).

<sup>8</sup>V. L. Granatstein, P. Sprangle, R. K. Parker, and M. Herndon, *J. Appl. Phys.* **46**, 2021 (1975).

<sup>9</sup>N. I. Zaytsev *et al.*, *Radiotekh. Elektron.* **19**, 1056 (1974).

<sup>10</sup>S. Humphries, T. J. Lee, and R. N. Sudan, *Appl. Phys. Lett.* **25**, 20 (1974).

<sup>11</sup>C. A. Kapetanakis, J. Golden, and F. C. Young, *Nucl. Fusion* **16**, 151 (1976).

<sup>12</sup>J. Golden and C. A. Kapetanakis, *Appl. Phys. Lett.* **28**, 3 (1976).

<sup>13</sup>J. A. Nation, *Rev. Sci. Instrum.* **41**, 1097 (1970).

<sup>14</sup>H. J. Doucet and J. Buzzi, private communication.